Multi-shell Diffusion MRI Provides Better Performance in Discriminating Parkinson's Disease

Silvia De Santis[1], Nicola Toschi[2,3], Derek K Jones[1], Claudio Lucetti[4], Stefano Diciotti[5], Marco Giannelli[6], and Carlo Tessa[7]

[1]CUBRIC Cardiff University, Cardiff, United Kingdom, [2]Medical Physics Section, Department of Biomedicine and Prevention, Faculty of Medicine, University of Rome "Tor Vergata", Italy, [3]Department of Radiology, A.A. Martinos Center for Biomedical Imaging, MGH and Harvard Medical School, Boston, MA, United States, [4]Division of Neurology Unit, Versilia Hospital, Lido di Camaiore (Lu), Italy, [5]Department of Electrical, Electronic, and Information Engineering "Guglielmo Marconi", University of Bologna, Cesena, Italy, [6]Unit of Medical Physics, Pisa University Hospital "Azienda Ospedaliero-Universitaria Pisana", Pisa, Italy, [7]Division of Radiology Unit, Versilia Hospital, Lido di Camaiore (Lu), Italy

PURPOSE AND TARGET: Parkinson's disease (PD) is a late-onset neurodegenerative disorder associated with motor progressive impairment that results from the death of dopamine-generating cells in the substantia nigra. While conventional, relaxometry-based brain MRI sequences are routinely applied in diagnostic settings in PD, more recently developed imaging techniques are being extensively tested to improve understanding of pathophysiologic changes, sensitivity to early disease onsets and specificity with respect to other neurodegenerative diseases such as atypical parkinsonisms. Diffusion tensor imaging (DTI) [1] has emerged as a promising tool to quantify microstructural damage in neurodegenerative disease. Changes in fractional anisotropy (FA) values can be measured throughout the brain in premotor PD, even when no significant atrophy is seen [2], although both sign and location of the change are inconsistent across studies. Increases in FA in frontal white matter [3-4], as well as decreases in FA in frontal lobes [5] and in nigrostriatal projection [6] have been observed. This lack of consistency could be addressed by resorting to more advanced metrics extracted from the diffusion decay by employing multi-shell techniques. Amongst them, only diffusional kurtosis has been applied to PD, demonstrating potentially increased diagnostic performance [7]. We aim at applying two more recent approaches, the composite hindered and restricted model of diffusion (CHARMED) [8] and the stretched exponential model (SEM) [9], to test the ability of multi-shell methods to differentiate between PD patients and healthy controls. Target audience is basic scientists interested in multi-shell diffusion MRI and clinical scientists interested in PD.

METHODS: 24 PD and 26 age- and gender-matched controls underwent diffusion MRI scanning using the following parameters: voxel size 2.8 mm isotropic, matrix 96x96x60, 2 b-value shells (b=1000 and 2500 s/mm^2) comprising 64 directions each, TE/TR=101/8500 ms. Data were corrected for motion and distortion using ExploreDTI [10] and processed using Matlab in-house scripts, to generate maps of the axonal density (from CHARMED) and of the stretching exponent (from SEM) as well as FA, and mean diffusivity (MD). Mean values and standard deviations for the two groups were obtained in 50 regions of interest (ROIs) obtained by combining the FA-derived skeleton from the tract-based spatial statistics pipeline with standardized white matter (WM) labels in standard space, as described in [11]. The mean values of all indices in the 50 ROIs were used in a binary classification analysis, which employed a multilayer perceptron algorithm (learning rate: 0.3, momentum: 0.2, 500 epochs, 2 layers) with a 10-fold cross validation strategy. No feature selection was performed. ROC curves were generated by varying the threshold on the class probability estimates. Classification analysis was performed in Weka v. 3.7 [12].

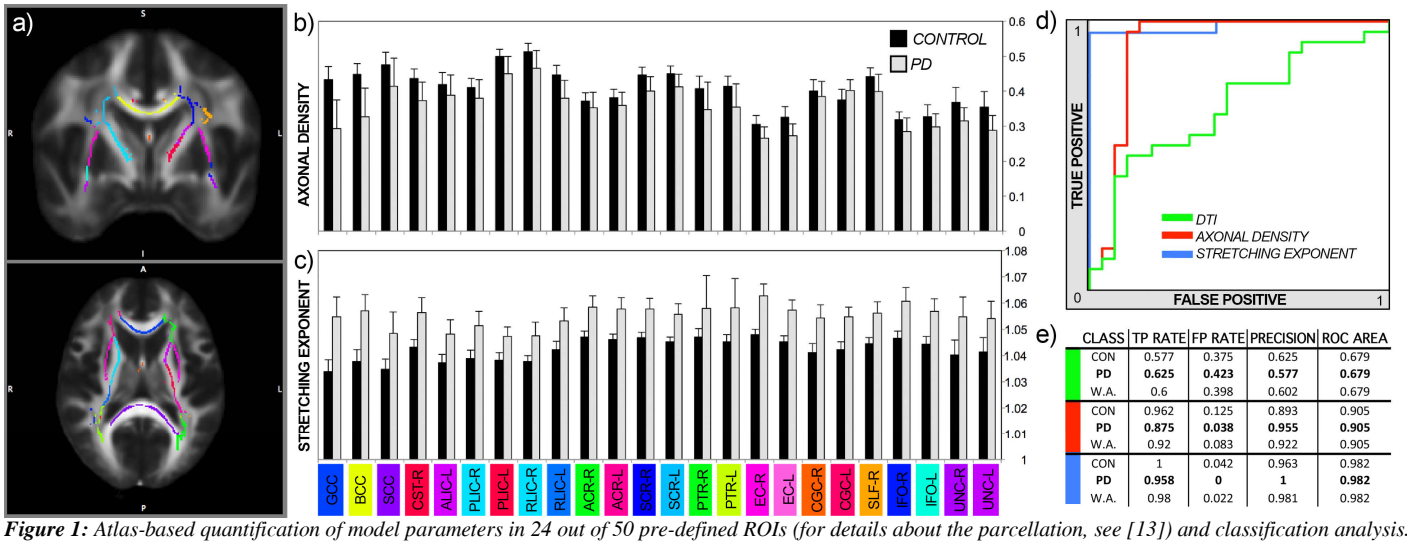

CLASS	TP RATE	FP RATE	PRECISION	ROC AREA
CON	0.577	0.375	0.625	0.679
PD	**0.625**	**0.423**	**0.577**	**0.679**
W.A.	0.6	0.398	0.602	0.679
CON	0.962	0.125	0.893	0.905
PD	**0.875**	**0.038**	**0.955**	**0.905**
W.A.	0.92	0.083	0.922	0.905
CON	1	0.042	0.963	0.982
PD	**0.958**	**0**	**1**	**0.982**
W.A.	0.98	0.022	0.981	0.982

Figure 1: *Atlas-based quantification of model parameters in 24 out of 50 pre-defined ROIs (for details about the parcellation, see [13]) and classification analysis. ROIs are shown in (a). Mean ROI-wise values of axonal density and stretching exponent all ROIs are shown in b) and c), respectively. ROC curves (PD vs controls) generated using the three models are shown in d). e) Provides details about classification analysis.*

RESULTS AND DISCUSSION: Employing ROI-wise indices extracted from multi-shell diffusion MRI resulted in extremely high classification performance when discriminating PD from control subjects (area under the ROC curve: 0.905 and 0.982 for the axonal density and for the stretching exponent, respectively). In contrast, DTI indexes performed poorly in the same classification task (area under the ROC curve using both FA and MD: 0.679). In all ROIs, axonal density was lower in PD patients as compared to controls, whereas the stretching exponent was found to be higher in PD as compared to controls. Since CHARMED is a microstructural model of WM, the reduction in axonal density can be interpreted directly as disruption of WM microstructure in PD. While the SEM showed the best performance in the classification task, its purely phenomenological approach to quantifying the deviation from Gaussian decay renders interpretation less straightforward. We speculate that the shape of the stretched exponential can be particularly suitable to uncover differences in microstructural organization caused by PD.

CONCLUSION: Multi-shell diffusion MRI provides significantly higher sensitivity and specificity to microstructural WM alterations in PD, which cannot be detected using conventional DTI. Employing more advanced models such as CHARMED or SEM to study neurodegenerative pathologies may aid the interpretation of otherwise aspecific differences which can be detected using conventional techniques such as DTI.

REFERENCES:

[1] Basser et al. *J Magn Reson B* **103** :247 (1994) [2] Tessa et al. *Am J Neuroradiol* **29**:674 (2008) [3] Haller et al. *Am J Neurorad* **33**;2123 (2012) [4] Skidmore et al *Neuroinformatics* (2014,in press) [5] Kendi et al. *Am J Neuroradiol* **29**:501 (2008) [6] Yoshikawa et al. *J Neurol, Neurosurg and Psychiatry* [7] Wang et al. *Radiology* **26**:210(2011) [8] Assaf and Basser *MRM* **52**:965 (2004) [9] Hall and Barrick, *MRM* **59**:447 (2008) [10] Leemans A et al. *Proc. ISMRM* (2009) [11] De Santis S et al. *Neuroimage* 89:35 (2014) [12] Hall et al SIGKDD *Explorations* 11 (2009) [13] Mori et al. *NI* **40**:570 (2008)